



ELSEVIER

Thermochimica Acta 367–368 (2001) 229–238

thermochimica  
acta

www.elsevier.com/locate/tca

# Heat capacity by sawtooth-modulated, standard heat-flux differential scanning calorimeter with close control of the heater temperature<sup>☆</sup>

Jeongihm Pak<sup>a,b</sup>, Bernhard Wunderlich<sup>a,b,\*</sup>

<sup>a</sup>Department of Chemistry, The University of Tennessee, Knoxville, TN 37996-1600, USA

<sup>b</sup>Chemical and Analytical Sciences Division, Oak Ridge National Laboratory, Oak Ridge, TN 37831-6197, USA

Received 15 October 1999; accepted 1 May 2000

## Abstract

Heat capacities are determined for the different frequencies generated as higher harmonics of the Fourier-transform of the heat-flow rate and sample temperature with quasi-isothermal, temperature-modulated differential scanning calorimetry (TMDSC). A complex sawtooth modulation was created using a TMDSC of the heat-flux type, controlled close to the heater. The complex sawtooth is designed to yield four harmonics of similar amplitudes. This new modulation method permits the determination of heat capacity with assurance of identical thermal history and sample geometry, which are important for the study of non-equilibrium processes as they exist, for example, in the glass transition region. Using a proper calibration by plotting the frequency dependence of the calorimeter response, heat capacities are determined approaching a 0.1% standard deviation for polymers. Best results were found for modulation with a complex sawtooth of 14 segments with a maximum amplitude of 1.0 K, a period of 420 s for 9–30 mg of polymer sample, and a sampling interval of one point per second. Published by Elsevier Science B.V.

*Keywords:* Sawtooth-modulated DSC; Poly(methyl methacrylate); Glass transition; Heat capacity

## 1. Introduction

The analysis of the glass transition is important in the characterization of thermal properties of polymers, and one of the most widely used technique to deter-

mine the glass transition is differential scanning calorimetry (DSC). The transition, however, depends on the thermal history of the sample [1] and during measurements in the glass transition region, the sample history changes. If one can measure simultaneously several heat capacities at different frequencies, this problem will be eliminated. The simultaneous use of multiple modulation frequencies was proposed already at the outset of development of the temperature-modulated DSC (TMDSC) [2], but seems not to have been applied to the measurement of heat capacity.

Recently, we attempted a series of standard DSC-experiments, modulated with a sawtooth-like change

<sup>☆</sup>The submitted manuscript has been authored by a contractor of the US Government under the contract No. DE-AC05-96OR22464. Accordingly, the US Government retains a nonexclusive, royalty-free license to publish, or reproduce the published form of this contribution, or allow others to do so, for US Government purposes.

\*Corresponding author. Present address: Department of Chemistry, The University of Tennessee, Knoxville, TN 37996-1600, USA. E-mail address: athas@utk.edu (B. Wunderlich).

of temperature, and analyzed the result by using the higher harmonics of the Fourier-transform. The initial experiments were based on a power-compensation type calorimeter [3]. In this new method all data of different frequencies are generated at once, so that the thermal history should be as identical as possible for all frequencies. The sawtooth-modulation was chosen because of its ease of generation by using an obvious variation of the program for a standard DSC. The Fourier series of a centro-symmetric sawtooth contains only odd numbered sinusoidal harmonics, i.e., it represents a convenient sum of sinusoidal modulations of different frequencies. The heat capacity of sinusoidally modulated samples in TMDSC is, in addition, easy to evaluate [4]. Unfortunately, however, the amplitudes of the higher harmonics decrease quickly with  $\nu$ , the order of the harmonic. This decrease in amplitude should lead to a diminished precision of the measurement. Despite the small amplitudes, it was possible to use up to the 11th harmonic to assess the frequency response of the calorimeter and to derive the characteristic relaxation times for the instrument [3].

In order to improve the precision of the analysis, a new, complex sawtooth-modulation was proposed [5]. It is generated by adjusting the 1st, 3rd, 5th and 7th harmonics of the sawtooth to equal amplitudes. The result was a complex sawtooth with 26 different linear segments. This complex sawtooth with 26 segments can be simplified without losing much of the similarity of the first amplitudes of the Fourier series by using only 14 segments, as listed in Table 1 and expressed by

$$T_b(t) - T_0 = A[0.3782 \sin \omega t + 0.2511 \sin 3\omega t + 0.2172 \sin 5\omega t + 0.3477 \sin 7\omega t - 0.0671 \sin 9\omega t \dots], \quad (1)$$

where  $T_b(t)$  is the program temperature,  $T_0$  the base temperature of the quasi-isothermal experiment,  $A$  the overall amplitude, and  $\omega$  the frequency in radian per second ( $=2\pi/p$ ,  $p$  representing the period in seconds).

In this paper, this simplified complex-sawtooth will be tested using a heat-flux DSC, as built by Mettler-Toledo, which is controlled close to the heater. Similar analyses with a heat-flux DSC controlled close to the sample temperature [6] and with a power-compensation DSC which is controlled at the heater position [7] were also carried out recently. Each of these differently constructed DSCs gives a different response to

Table 1  
Complex sawtooth program for  $p = 420$  s

Segment No. <sup>a</sup>	Time (s)	Amplitude (K)
1	0–15.0	0.0–1.0
2	15.0–45.0	1.0–0.0
3	45.0–75.0	0.0–0.5
4	75.0–105.0	0.5–0.0
5	105.0–135.0	0.0–0.5
6	135.0–165.0	0.5–0.0
7	165.0–195.0	0.0–1.0
8	195.0–225.0	1.0 to –1.0
9	222.5–255.0	–1.0–0.0
10	255.0–285.0	0.5 to –0.5
11	285.0–315.0	–0.5–0.0
12	315.0–345.0	0.0 to –0.5
13	345.0–375.0	–0.5–0.0
14	375.0–405.0	0.0 to –1.0
15	405.0–420.0	–1.0–0.0

<sup>a</sup> Note that in order to keep a centro-symmetric sawtooth, segments 1 and 15 are half segments.

the modulation with the complex sawtooth and needs specific analysis and calibration methods to reach peak performance.

The amplitude for each harmonic  $\nu$  of the heat-flow rate  $A_{HF}$  and the sample temperature  $A_{T_s}$  from a quasi-isothermal measurement with the complex sawtooth yields the heat capacity ( $C_p$ ) as

$$C_p = \frac{A_{HF}(\nu)}{A_{T_s}(\nu)} \frac{1}{\omega'} K(\omega'), \quad (2)$$

where  $\omega' = \omega \times \nu$ , with  $\nu = 1, 3, 5, 7$  and  $9$ , the numbers of the harmonics considered.

The calibration function  $K(\omega')$  was originally derived for sinusoidally modulated heat-flux calorimetry under the conditions of steady state and a negligible temperature gradient within the sample [8]. In this case  $K(\omega')$  is  $[1 + (C_r \omega' / K)^2]^{0.5}$ , with  $C_r$  representing the heat capacity of the reference calorimeter and  $K$  the Newton's law constant. In sawtooth modulation, steady state is lost every time the heating rate changes abruptly. But it could be shown that as long as the heat-flow rate is described by a linear differential equation, such as the Fourier equation for heat flow, steady state is not required for the use of Eq. (2) with the indicated correction factor for the differences in sample and reference calorimeter [9]. To study any other dependencies, such as on sample and reference material, contact resistance and possible

temperature gradients in the sample, an empirical expression was suggested to obtain useful data from Eq. (2) [4]:

$$K(\omega') = \sqrt{1 + \tau^2(\omega')^2}, \quad (3)$$

where  $\tau$  is a constant, whose characteristics are to be established empirically. The value for  $\tau$  in Eq. (3) can be obtained by plotting the inverse of the squared, uncorrected heat capacities of Eq. (2) which are computed by setting  $K(\omega') = 1$  versus the square of the frequency [4]. If this procedure yields a linear function,  $\tau$  is independent of  $\omega'$  and can be determined from the slope of the curve and the corrected heat capacity is given by the intercept. With the present calorimeter, it will be shown that a quadratic function yields a somewhat better fit. The corrected heat capacity is still to be calibrated by comparison with a measurement of a calibrant, such as sapphire, under identical conditions. To correct for the asymmetry of the differential calorimeter, a baseline correction is needed for the measurement of the sample and the calibrant. Commonly this is done in the time domain before the Fourier analysis (but see also the comments on this method in [5]).

In this paper this simultaneous measurement of heat capacity with several modulation frequencies in response to a simple sawtooth is analyzed with a heat-flux type TMDSC with temperature control close to the heater, as done before on a power-compensation DSC [3], but the main issue is the application of the new complex sawtooth modulation of Eq. (2). Modulation frequencies, sample mass, and sampling frequency are varied to find a best performance. It is proven that it is possible to reach a 0.1% precision with a temperature-modulated DSC.

## 2. Experimental

### 2.1. Instrumentation

Apparent heat capacity measurements were carried with a heat-flux type Mettler-Toledo DSC 820<sup>TM</sup> with the FRS-5 sensor. In this DSC, temperature is measured close to the furnace body and used to control the modulation and also to establish the reference temperature. In addition, the temperature difference

between reference and sample is measured by the heat-flux sensor FRS-5. Dry N<sub>2</sub> gas with a flow rate of 20 ml min<sup>-1</sup> was purged through the DSC cell in the instrument. Cooling was accomplished with a liquid-nitrogen cooling-accessory. The temperature scale was calibrated at a heating rate of 10 K min<sup>-1</sup> in the standard DSC-mode using the onset melting temperatures for the following substances: tin (505.08 K), indium (429.75 K), H<sub>2</sub>O (273.15 K), and *n*-octane (217.39 K). An initial calibration of the heat-flow rate was done with the heat of fusion of indium (28.45 J g<sup>-1</sup>) and the heat capacity of the sample poly(methyl methacrylate) (PMMA) was then recalibrated with sapphire, measured immediately before each sample run.

### 2.2. Simple sawtooth modulation

Quasi-isothermal TMDSC [10] (with an underlying heating rate  $\langle q \rangle = 0$ ) was done first with a simple sawtooth at 300 and 450 K. Periods  $p$  of 30–600 s were chosen, all with a modulation amplitude of 1.0 K. The 1st, 3rd, 5th, 7th and 9th harmonics were evaluated for all modulations, yielding information on periods from 3 $\frac{1}{3}$  to 600 s. A total of 12 experiments was performed, seven with sapphire, five with PMMA. Some of these runs were carried out under conditions of a defective cooling system, which was discovered after a part of this set of measurements was completed, but the data were still useable, although the  $\tau$ -values changed.

### 2.3. Complex sawtooth modulation

The complex sawtooth was programmed as listed in Table 1 with  $p = 420$  s. Experiments with proportionally adjusted modulations with  $p = 210, 280$  and 840 s were also performed using sapphire as a test material. For the 420 s complex sawtooth, the length of each segment is 30 s. The periods for the higher harmonics with  $v = 1, 3, 5, 7$  and 9 are 420, 140, 84, 60 and 46 $\frac{2}{3}$  s, respectively. The 9th harmonic is not adjusted to a similar amplitude, but since it has contributions from the adjusted 1st and 3rd harmonic, its amplitude is eight times larger than the Fourier series of a simple sawtooth [5]. All higher harmonics were considered too small in amplitude for analysis. All measurements were made in the quasi-isothermal

mode at temperatures of 300 or 450 K. In every experiment, the complex sawtooth was repeated seven times. Data from cycles 3–6 were collected for evaluation. Three sequential runs were done to obtain data for reference (sapphire versus an empty pan), for the baseline (with two empty pans), and the sample (sample versus an empty pan). The Fourier analysis was carried using the software supplied with the calorimeter by Mettler-Toledo (analysis technique 5.1). A total of 34 runs was made for PMMA and sapphire under varying conditions to establish a recipe for best precision. At 300 K, the best condition can be summarized as using a fully adjusted calorimeter with optimum cooling performance, a period of 420 s for the complex sawtooth with an amplitude of 1.0 K, 9–30 mg of polymer sample, and a sampling interval of  $1.0 \text{ s}^{-1}$ .

#### 2.4. Sample and pan

The reference sample is an  $\text{Al}_2\text{O}_3$  single crystal disc (sapphire) of 22.564 mg. The atactic PMMA was a secondary standard of Aldrich. It had a weighted-average molar mass of 102 600 Da, and number-average molar mass of 48 300 Da. The glass transition of PMMA is about 378 K. The samples came powdered and were pressed above the glass transition tempera-

ture into a film to increase thermal contact. Weighing was done on a Cahn C-33 electrobalance to  $\pm 0.0005 \text{ mg}$ . The flat-bottom reference and sample pans (around 48 mg) were kept in the same position in the calorimeter for all three sequential measurements. The sample was moved in and out of the empty pan without crimping the lid. The empty reference pan was always the same and had a mass of 46.044 mg.

#### 2.5. Data treatment

The heat-flow rate of the baseline run was subtracted from the sample run in the time domain to approximately correct for the asymmetry of the equipment. A typical set of heat-flow rate data for the complex sawtooth of Table 1 for a sample and baseline run is depicted in Fig. 1. The curves are automatically smoothed by the manufacturer's software. The sampling intervals are 0.5 s per point. Only four cycles (3rd–6th) of the experimental data of the heat-flow rate and the sample temperature were analyzed using the software provided by the manufacturer. The obtained amplitudes for each harmonic  $\nu$  of the heat-flow rate ( $A_{\text{HF}}$ ) and the sample temperature ( $A_{T_s}$ ) were transferred as ASCII data to a PC and the specific heat capacity,  $C_p$ , was evaluated using the commercial Sigma Plot<sup>TM</sup> program version 4.00.

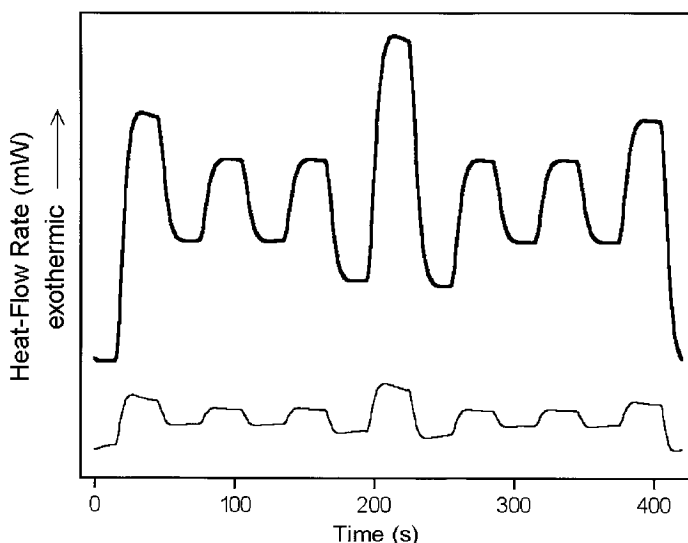


Fig. 1. An example of the as-measured heat-flow data for sapphire and a baseline run. The heavy line refers to sapphire, the thin line represents the baseline (an empty pan measured versus an empty pan).

### 3. Results

#### 3.1. Simple sawtooth modulation

The raw data of the heat-flow rate and the sample temperature of a simple sawtooth are illustrated in Fig. 2. The modulation occurs about the base temperature ( $T_0 = 300$  K) with an amplitude of 1.0 K and a period of 30 s (left-hand side part of the figure) and 120 s (right-hand side part) which yield temperature changes of 8 and 2 K  $\text{min}^{-1}$ , respectively. The sample-temperature profile is that of a centrosymmetric sawtooth and closely follows the programmed temperature. It takes 17–23.5 s for the heat-flow rate to reach steady state which is required for a heat capacity calculation using the standard DSC equation:

$$C_p \approx \frac{\langle \text{HF} \rangle}{\langle q \rangle}, \quad (4)$$

where  $\langle \text{HF} \rangle$  and  $\langle q \rangle$  are the steady-state heat flow and heating rates of the sawtooth.

With a sufficiently low frequency, one can thus evaluate the average of the horizontal portion of the heat-flow rate with Eq. (4). With the 30 s period, as on the left curves of Fig. 2, steady state is never reached since each half-cycle has only 15 s for its completion, i.e., only Eq. (2) can be used for the analysis.

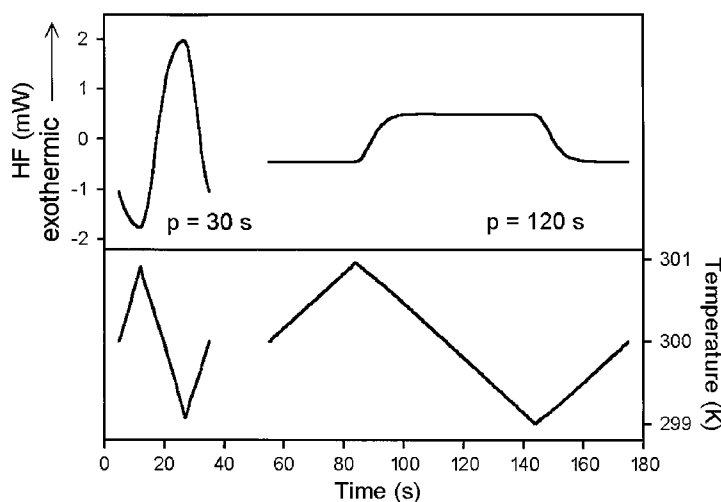


Fig. 2. Heat-flow rates (top) and sample temperatures (bottom) as a function of time for quasi-isothermal, simple sawtooth modulation ( $p = 30$  and 120 s,  $T_0 = 300$  K, sapphire disc of 22.564 mg).

Fig. 3a shows typical data for sapphire, modulated at 120 and 480 s after calculation of the uncorrected, apparent heat capacities with Eq. (2) ( $\nu = 1-9$ ,  $K(\omega') = 1$ ; symbols: (○) and (Δ), respectively). Both sets of data follow the same functional relationship. Next, as suggested by Eq. (3), the inverse squares of the uncorrected specific heat capacities are plotted versus  $(\nu\omega)^2$ , as shown in Fig. 3b. The harmonics with periods larger than 40 s ( $(\nu\omega)^2 < 0.025$ ) can be represented by the straight line, indicated in Fig. 3b with a constant  $\tau$  of 2.67 s  $\text{rad}^{-1}$ . The  $R^2$  of the line is 0.969. Applying the correction of Eq. (3), the specific heat capacities for different frequencies converge in Fig. 3a into the horizontal, dotted line (symbols (●) and (▲)). Below 40 s, however, this correction does not apply, as can be seen by the deviations from the straight line in Fig. 3b and the three shaded circles in Fig. 3a (5th, 7th and 9th harmonic of the sawtooth with  $p = 120$  s). The change of  $\tau$  with the square of the frequency is, however, a continuous function and can be fitted well with a quadratic function, allowing then to include also data below 40 s into the analysis as will be summarized next.

The heavy line in Fig. 3a is the expected specific heat capacity of sapphire at 300 K, as listed in Ref. [11]. The dotted line represents the average of the corrected specific heat capacities. The deviation from

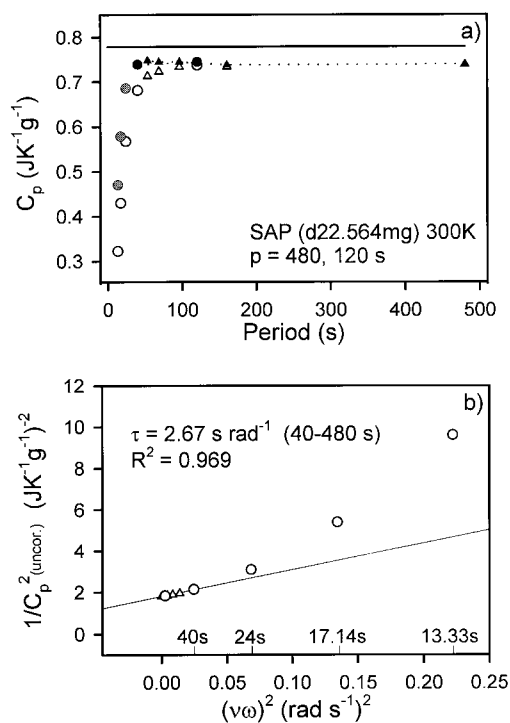


Fig. 3. (a) Specific heat capacity of sapphire as a function of the modulation period for simple sawtooth modulation.  $T_0 = 300$  K,  $p = 480$  and  $120$  s. Open symbols represent the calculated data for the 1st–9th harmonic of a Fourier fit using Eq. (2) with  $K(\omega') = 1$  (uncorrected). Filled symbols are corrected according to Eq. (3) with  $\tau = 2.67$  s  $\text{rad}^{-1}$ , derived in Fig. 3b. Shaded circles did not lead to acceptable corrections with a linear fit. (b) Square of the inverse uncorrected specific heat capacity (open symbols in Fig. 3a) of sapphire as a function of the square of the modulation frequency.

the heavy line yields the calibration factor. The standard deviation of the data points represented by all filled symbols in Fig. 3a is 0.52%. The average standard deviation of the specific heat capacities calculated from the 1st, 3rd, 5th, 7th and 9th harmonic of seven simple sawtooth experiments at 300 and 450 K for sapphire and PMMA, with periods ranging from 400 to 600 s was 0.36%. Extending the fit to a quadratic equation, the average standard deviation for nine experiments with periods from 240 to 600 s could be reduced to 0.28%. Similar improvements were possible by excluding some higher harmonics as was done in Fig. 3b for the linear fit to obtain  $\tau$ . Using the quadratic fit for the data of Fig. 3b which combines the 120 and 480 s sawtooth results and excluding

points below 40 s yields a standard deviation of 0.22%.

### 3.2. Complex sawtooth modulation

Even though the higher harmonics of the simple sawtooth give still heat capacity data, the amplitudes of the higher harmonics decrease. Fig. 4 illustrates the 14 segments of the complex sawtooth of Table 1 which is designed to avoid this disadvantage for the simple sawtooth. The top curve illustrates the heat-flow rate after baseline subtraction. It is for the sapphire disc of 22.564 mg at 300 K. The overall period was chosen to be 420 s with  $\nu = 1, 3, 5, 7$  and 9, corresponding to periods of the harmonics of 420, 140, 84, 60 and  $46\frac{2}{3}$  s, so that all sub-segments could reach steady state before changing to the next sub-segment. The 9th harmonic is longer than 40 s, the limit of linear fitting in Fig. 3b. All five specific heat capacity data of the complex sawtooth should thus fit the analysis with a frequency-independent  $\tau$ . The (barely visible) dotted line in the bottom curve is the programmed temperature and the solid one is the actual sample temperature. The calorimeter follows the sawtooth very closely. Also, since the upper curve reaches steady state at the end of each sub-segment, one can calculate the heat capacity using the standard DSC Eq. (4).

The uncorrected specific heat capacities are indicated in Fig. 5a (symbol: (○)). In the larger scale of Fig. 5b, one can see that the five inverse-squared, uncorrected specific heat capacities fit a quadratic function better than a linear one, even at low frequency, i.e., the time constant  $\tau$  is not constant with frequency. Using the quadratic fit, precise specific heat capacity data can be generated, as shown by the filled circles in Fig. 5a (symbol: (●)). The standard deviation of the corrected data is 0.13%. The calibration factor is 1.04. Fig. 5a shows also the standard DSC data from the horizontal portions of the steady-state regions using Eq. (4). The triangles represent the specific heat capacities thus calculated.

The specific heat capacities of PMMA in Fig. 6a are obtained using the same complex sawtooth modulation as the sapphire and baseline runs discussed in Figs. 4 and 5. The triangles are again the heat capacities calculated using standard DSC equation. The solid line represents the specific heat capacity data PMMA as can be derived from the ATHAS data-bank

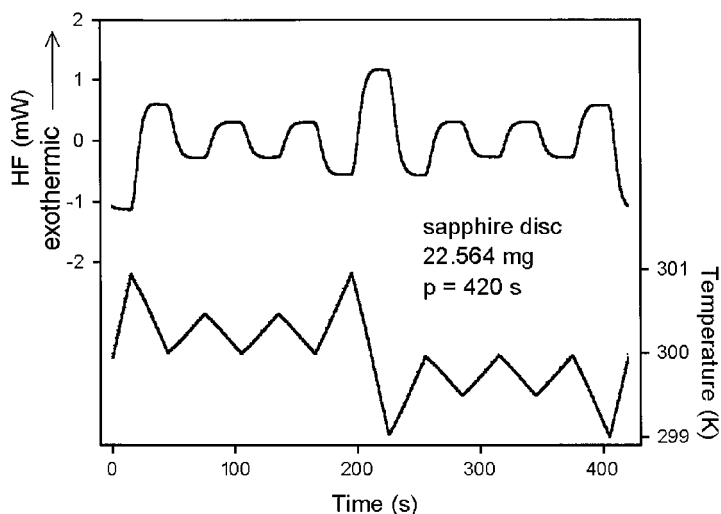


Fig. 4. Heat-flow rates (top) and the sample temperatures (bottom) as a function of time for quasi-isothermal, complex sawtooth modulation ( $p = 420$  s,  $T_0 = 300$  K). Measurement of a disc of sapphire of 22.564 mg.

[12]. The filled circles are the specific heat capacities corrected for frequency and then calibrated with a sapphire run. They deviated by  $+0.76\%$  from the literature data and had a standard deviation about the mean of  $0.04\%$ . Note, however, that the data-bank data are commonly not more precise than  $\pm 3\%$ .

Excluding a number of runs that were made under imperfect cooling conditions due to an instrument defect that was discovered and corrected during the research, only eight runs with 22.564 mg sapphire and complex sawtooth modulations of 210, 420 and 840 s periods at 300 K led to an average standard deviation of  $0.36\%$ . Selecting only the four runs with 420 s complex sawtooth modulations, the average standard deviation was  $0.10\%$ .

Under similar conditions as just discussed, four runs of PMMA of masses ranging from 3.711 to 31.727 mg led to an average standard deviation of  $0.11\%$ . The three best results with masses above 9 mg of PMMA gave an average standard deviation of  $0.06\%$  (see Fig. 6). As expected, measurements of solid, well-fitting discs placed in the sample pan gave best results (standard deviation,  $0.22\%$ ), followed by fine powders ( $0.51\%$ ), and larger, irregular particles ( $0.58\%$ ), all of the same mass of about 22.5 mg of sapphire. Similarly, best data were obtained with sapphire using sampling intervals of 1.0 s or less (average of  $0.16\%$  for the standard deviation of four experiments).

#### 4. Discussion

Figs. 3, 5 and 6 demonstrate that optimized TMDSC can approach a  $0.1\%$  precision in measuring heat capacity, while the standard DSC carried out under the same conditions remains at the level established earlier [13]. In this earlier study of the heat capacity of liquid selenium, the three most prominent commercial calorimeters could measure to better than  $\pm 3\%$ . It should be noted, however, that the present measurements were not optimized for the standard DSC. Earlier, extensive efforts to calibrate the standard DSC also let us to believe that even standard DSC could approach the  $0.1\%$  mark of precision when all heat losses and instabilities could be eliminated or corrected for [14]. The modulated DSC provides the elimination of many of the major sources of error by extracting only heat-flow signals which have the same frequency of modulation as the corresponding sample-temperature modulation. The present experiments have illustrated also that the common needs of stability of the calorimeter and consecutive calibrations are necessary. It is, thus, still a major effort to measure heat capacity to better than  $3\%$ .

The analysis of a simple sawtooth using the higher harmonics with their decreasing amplitudes is documented with Figs. 2 and 3. Such investigation was also carried out with a power-compensated DSC [3].

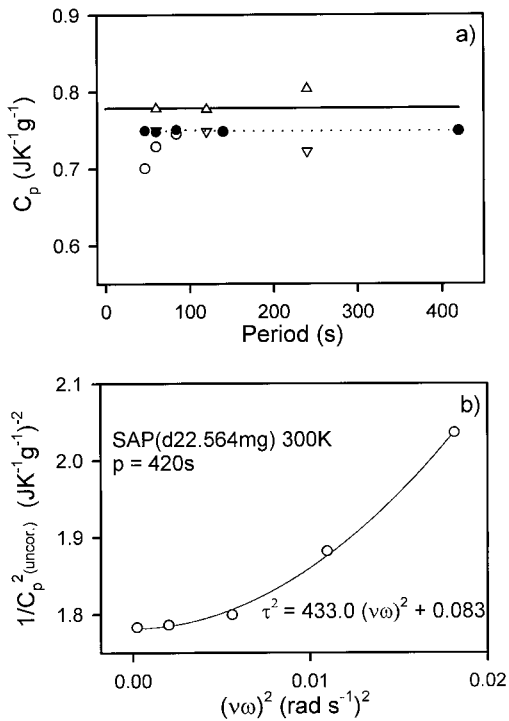


Fig. 5. (a) Specific heat capacity of sapphire for a complex sawtooth modulation (data of Fig. 4) with  $p = 420$  s,  $T_0 = 300$  K. Open circles ( $\circ$ ), calculated for the 1st–9th harmonics of a Fourier fit using Eq. (2) with  $K(\omega') = 1$  (uncorrected). Filled circles ( $\bullet$ ), corrected according to Eq. (3) with  $\tau$  from the quadratic fitting in Fig. 5b. Triangles ( $\Delta$  and  $\nabla$ ) are calculated using the standard-DSC equation (Eq. (4)) on heating and cooling, respectively. (b) Square of the inverse, uncorrected specific heat capacity of sapphire ( $\circ$  in Fig. 5a) as a function of the square of the modulation frequency.

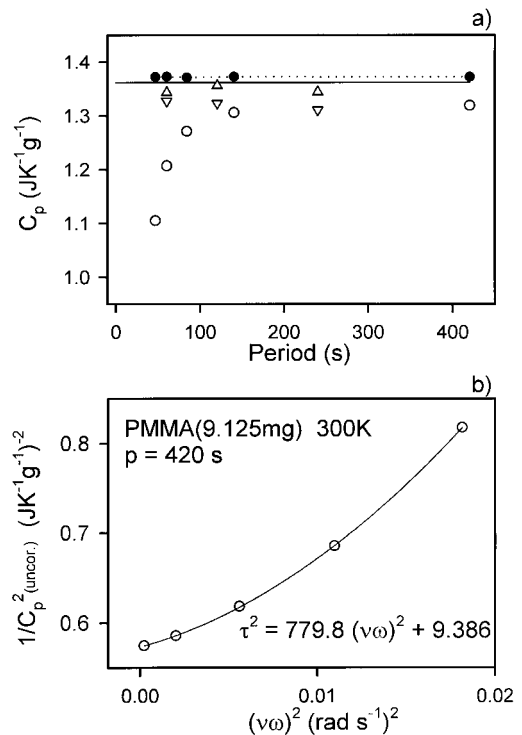


Fig. 6. Specific heat capacity of PMMA for a complex sawtooth modulation 9.125 mg with  $p = 420$  s,  $T_0 = 300$  K. Open circles ( $\circ$ ), calculated for the 1st–9th harmonics of a Fourier fit using Eq. (2) with  $K(\omega') = 1$ . Filled circles ( $\bullet$ ), corrected according to Eq. (3) with  $\tau$  from the quadratic fitting in Fig. 6b. Triangles ( $\Delta$  and  $\nabla$ ) are calculated using the standard-DSC equation, Eq. (4), on heating and cooling, respectively. (b) Square of the inverse, uncorrected specific heat capacity of PMMA ( $\circ$  in Fig. 6a) as a function of the square of the modulation frequency.

Furthermore, it was linked here for the analyzed Mettler-Toledo ADSC<sup>TM</sup> to a simple model calculation [15]. Both the prior and the present investigations indicate that it is possible to obtain better data when using TMDSC than with the standard DSC. In order to accumulate sufficient data points and to overcome the decreasing amplitudes with frequency of the simple sawtooth, experiments with several periods  $p$  may be necessary. The precision of 0.25–0.5% achieved in these measurements is already considerably better than for the standard DSC. It can be seen in Fig. 2 that a segment of the sawtooth of length 15 s is too short to reach the steady state for  $A_{T_s} = 1.0$  K and  $p = 30$  s. Using the higher harmonics of the sawtooth allows to extract data for a period of  $3\frac{1}{3}$  s, which

corresponds to the 9th harmonic of a simple sawtooth with a period of 30 s. The strong frequency dependence of the uncorrected heat capacities must naturally be corrected for, as shown in Fig. 3. The linear relationship found often to be sufficient in other calorimeters [3,6,7] has a limit of 0.025 Hz in the case of the Mettler-Toledo DSC 820 ( $0.16 \text{ rad s}^{-1}$ ,  $p = 40$  s), but the higher frequencies follow still a functional relationship that is easily fitted.

Turning to the complex sawtooth of Fig. 4, one can see the very close fit to the program of Table 1. Such a good fit is always observed when the temperature is controlled close to the heater [7]. The sum of the 1st to the 9th harmonic make use of most of the experimental information, so that the use of even higher harmonics



Table 2  
Temperature amplitudes and ratios of the various harmonics of the complex sawtooth of Fig. 4<sup>a</sup>

Number of the harmonics, $\nu$	Amplitude of $T_s$ (K)		Ratio of $A_{HF}$ to $(A_{T_s} \times \nu)$	
	Simulation and programmed	Measured	Simulation <sup>b</sup>	Measured
1 <sup>st</sup>	0.37819	0.3776	0.02992	0.3146
2 <sup>nd</sup>	$1.5 \times 10^{-6}$	$2 \times 10^{-4}$	–	–
3 <sup>rd</sup>	0.25112	0.2478	0.02992	0.3099
5 <sup>th</sup>	0.21721	0.2099	0.02991	0.3054
7 <sup>th</sup>	0.34771	0.3265	0.02991	0.2995
9 <sup>th</sup>	0.06711	0.0609	0.02989	0.2923

<sup>a</sup> For the simulation data see Ref. [5],  $p = 210$  s, the measured data are for  $p = 420$  s.

<sup>b</sup> For the simulation data, the ratio is the amplitude of  $dT_s/dt$  divided by the amplitude of  $T_s \times \nu$ .

is not expected to yield better results [6,7]. Numerical values for the harmonics of the complex sawtooth are compared in Table 2. The Lissajous figure of the four averaged cycles analyzed can be seen in Fig. 7. Repeatability exists within the thickness of the lines of the figure. It is clear that the amplitudes of the second harmonic (and all other even-numbered harmonics) are close to zero, indicating that the centrosymmetric modulation of the program is maintained in the amplitudes of temperatures and heat-flow rates, as also proven by Fig. 7. The absolute values of the amplitudes decrease from the expected values slowly with frequency, as does the ratio needed for insertion

into Eq. (2). These changes lead to the frequency dependence of the uncorrected heat capacity seen in Figs. 5 and 6. The simulation data in column three could be corrected with a frequency and mass independent  $\tau$  of  $C_p/K$  [5], as discussed in Section 1. Its correction accounted only for the difference in heat flux between sample and reference calorimeter [9]. The additional effects seen in the experimental ratios are due to thermal conductivity effects that change with mass, sample type, and packing differences and disappear on extrapolation to frequency zero.

The frequency range over which  $\tau$  is constant with frequency decreases in going to the complex sawtooth

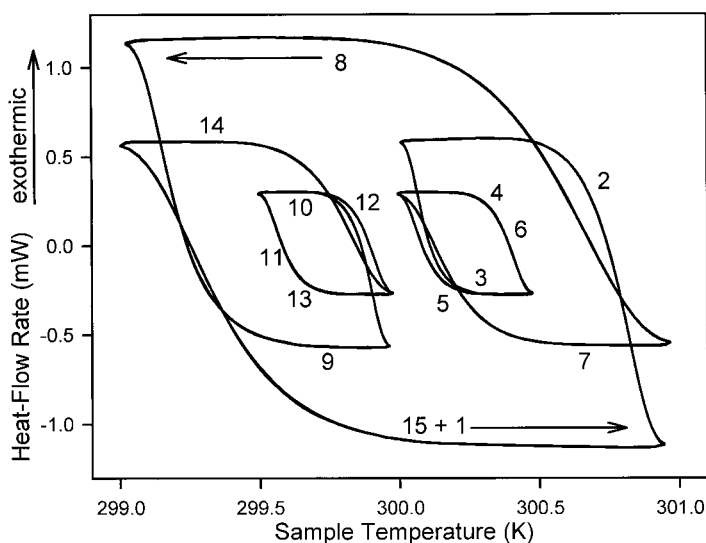


Fig. 7. Lissajous figure of the heat-flow rate plotted versus the sample temperature for the four cycles used for analysis (3rd–6th). Data of Fig. 4. The numerals refer to the segment numbers in Table 1.

(compare Figs. 3 and 5). It is difficult to pinpoint the cause of this change, but we expect that it is linked to the software that controls the heating rate and the smoothing of the data. It was shown, for example, in [7] that changes in the amount of smoothing considerably alter the value of  $\tau$ . As long as the changes in  $\tau$  can be described by a simple continuous equation, the extrapolation to zero frequency is possible and good quality heat capacities can be obtained. The value of  $\tau$  in itself has no particular meaning if data smoothing occurs. In the case of the Mettler-Toledo ADSC<sup>TM</sup>, small spikes of a heat-flow rate imbalance can occur when changing the heating rate. They are largely smoothed and also diminished on baseline subtraction. In addition, the smoothing routine of Mettler-Toledo has a variable number of consecutive data points, depending on the absolute change of the heat-flow relative to the noise level in the range of smoothing. Such type of smoothing causes unknown effects in the Fourier separation of higher harmonics. It may be of advantage to bypass the smoothing.

## 5. Conclusions

The work described in this paper was an effort to test the limits of measurement of heat capacity of polymers with quasi-isothermal TMDSC using frequencies with periods from  $3\frac{1}{3}$  to 840 s at an amplitude of 1 K. The goal has been reached to establish the parameters needed to make measurements of heat capacity approaching a precision of 0.1%. In the future, the obtained information is also to be used to study the frequency dependence of heat capacity in transitions like the glass transition to improve on the first results obtained earlier [16–21].

## Acknowledgements

This work was supported by the Division of Materials Research, National Science Foundation, Polymers Program, Grant # DMR-9703692 and the Division of Materials Sciences, Office of Basic Energy

Sciences, US Department of Energy at Oak Ridge National Laboratory, managed by Lockheed Martin Energy Research Corporation for the US Department of Energy, under contract No. DE-AC05-96OR22464.

## References

- [1] E. Turi (Ed.), *Thermal Characterization of Polymeric Materials*, Vol. 1, Academic Press, San Diego, CA, 1997 (Chapter 3).
- [2] M. Reading, B.K. Hahn, B.S. Crowe, Method and apparatus for modulated differential analysis, US Patent 5 224 775 (July 6, 1993).
- [3] R. Androsch, B. Wunderlich, *Thermochim. Acta* 333 (1999) 27.
- [4] R. Androsch, I. Moon, S. Kreitmeier, B. Wunderlich, *Thermochim. Acta* 357/358 (2000) 276.
- [5] B. Wunderlich, R. Androsch, M. Pyda, Y.K. Kwon, *Thermochim. Acta* 348 (2000) 181.
- [6] M. Pyda, Y.K. Kwon, B. Wunderlich, *Thermochim. Acta*, this issue.
- [7] Y.K. Kwon, R. Androsch, M. Pyda, B. Wunderlich, *J. Therm. Anal. Calorimetry*, this issue.
- [8] B. Wunderlich, Y. Jin, A. Boller, *Thermochim. Acta* 238 (1994) 277.
- [9] B. Wunderlich, A. Boller, I. Okazaki, K. Ishikiriyama, W. Chen, M. Pyda, J. Pak, I. Moon, R. Androsch, *Thermochim. Acta* 330 (1999) 21.
- [10] A. Boller, Y. Jin, B. Wunderlich, *J. Therm. Anal.* 42 (1994) 307.
- [11] D.G. Archer, *J. Phys. Chem. Ref. Data* 22 (1993) 1441.
- [12] Advanced thermal analysis system for downloadable data. <http://web.utk.edu/~athas/databank/acryl/pmma/pmmca-lam.html>.
- [13] A. Mehta, R.C. Bopp, U. Gaur, B. Wunderlich, *J. Therm. Anal.* 13 (1978) 197.
- [14] H. Suzuki, B. Wunderlich, *J. Therm. Anal.* 29 (1984) 1369.
- [15] I. Moon, R. Androsch, B. Wunderlich, *Thermochim. Acta* 357/358 (2000) 319.
- [16] B. Wunderlich, I. Okazaki, *J. Therm. Anal.* 49 (1997) 57.
- [17] I. Okazaki, B. Wunderlich, *J. Polym. Sci. B* 34 (1996) 2941.
- [18] L.C. Thomas, A. Boller, I. Okazaki, B. Wunderlich, *Thermochim. Acta* 291 (1997) 85.
- [19] A. Boller, I. Okazaki, B. Wunderlich, *Thermochim. Acta* 284 (1996) 1.
- [20] B. Wunderlich, A. Boller, I. Okazaki, S. Kreitmeier, *J. Therm. Anal.* 47 (1996) 1013.
- [21] A. Boller, C. Schick, B. Wunderlich, *Thermochim. Acta* 266 (1995) 97.